

Design and Analysis of High Gain Dual-polarized Dipole Antenna Based on Partially Reflective Metasurface

Chenqi Li^{1†}, Zhongsen Sun^{1†}, Zhejun Jin¹, Tian Liu¹, Leonid F. Chernjgor^{1,2},
and Yu Zheng^{1,*}

¹ College of Electronic Information, Qingdao University, Qingdao, 266071, China

² Department of Space Radiophysics, V.N. Karazin Kharkiv National University, Kharkiv, 61022, Ukraine

[†] These authors contributed equally to this work, *zhengyu@qdu.edu.cn

Abstract — A partially reflective metasurface (PRMS) structure is proposed for dual-polarized dipole antenna with a high gain and wide broadband. Stable radiation patterns are realized by using quadrilateral bottom reflector. The phase bandwidth of PRMS structure reflection presented in this paper matches well with the antenna operating bandwidth. The gain of the dual-polarized antenna is improved to 10.2dBi at 1.8GHz by adjusting the size and height of PRMS structure. Meanwhile, the bandwidth is expanded (61.2%). Measured result demonstrates that the antenna has a stable beamwidth which is desirable in base station applications. Furthermore, the designed antenna can be used for communication in complex environment because of its excellent performance.

Index Terms — Dual-polarize, high gain, partially reflective metasurface (PRMS), quadrilateral bottom reflector.

I. INTRODUCTION

Recently, with the increasing complexity of the electromagnetic application, high-gain antennas are widely used in base station backhaul and direction-finding systems to compensate the communication link loss. In addition, the dual-polarized property is also necessary for base station antenna to obtain minute interference and extensive channel capacity. Designing an antenna with high gain and dual-polarized property will play a significant role in the many wireless system.

The base station antenna types are primarily divided into patch class, dipole class and gap class [1]. The patch antenna and slot antenna is simple to manufacture, but the bandwidth is difficult to expand. With the benefits of high isolation and stable radiation pattern, the dipole antenna is the widely used form. For example, a novel double-polarized dipole antenna unit which working frequency band is 1.7 GHz to 2.7GHz is proposed and high relativity gain (8.5dBi) is obtained [7]. However, the proposed antenna size (200×130 mm)

limits its use as a base station cell. Using the differentially fed form, dual-polarized slot antenna realized high isolation and wide impedance bandwidths (19.3%). Nevertheless, the antenna structure is complex has a complicated structure, and the performance is hard to improve. Therefore, it is a meaningful challenge to increase the antenna gain and bandwidth with reduced antenna size.

Many research has proved that the new materials, such as frequency selective surface structures (FSSs), find wide applications in various antennas, radars (RCS reduction), and electromagnetic wave absorbers due to their many extraordinary properties [8-11]. The metamaterial structure can manipulate and control the surface distribution of electromagnetic waves by changing the geometry and alignment of the FSS to make the antenna obtain fine performance. Metamaterial structure is used as a partially reflective surface (PRS) which achieves an effect similar to a focusing lens. By selecting an artificial electromagnetic material to constitute a Fabry-Perot resonant antenna, a high gain and highly directional antenna was proposed in [12,13]. Moreover, thin subsurface is used in [14,15], which is improve the performance of circularized array antenna. In [16,17], the metamaterial reflective surface plays an important role for both single-feed circularly polarized antenna and microstrip patch antenna. As a result, the antennas obtain high gain and wide bandwidth. A partial reflector is also designed in [18] to make the antenna achieve dynamic control of beam width, which benefits from stable radiation pattern and high directivity. Therefore, the PRS, which has a compact structure, has been widely used to improve antenna performance. However, owing to the narrow reflection phase bandgap of metamaterial structure, it is difficult to integrate the antenna unit cell with the PRS while designing a high-gain base station antenna. Adding air dielectric layer maybe is an efficiency way to broaden the phase bandwidth of PRS structure [22].

In the present paper, we introduce the dual-polarized

dipole antenna with good performance that uses a metasurface structure with periodic arrays consisting of FSS and PRS for enhancing the gain and bandwidth. Also, an LC equivalent circuit model is used to demonstrate the feasibility of a partially reflective metasurface structure (PRMS). The measured results are in good agreement with the simulation results. By adjusting metasurface structure, the bandwidth is increased by 15.8%. Meanwhile, the maximum gain is increased by 4.9dBi at 2.8GHz. Moreover, the plane reflector is also modified.

II. DESIGN AND CONFIGURATION OF ANTENNA AND PRMS

A. Design of antenna and bottom reflector

A dual-polarized dipole antenna fed by two baluns is chosen as the primary antenna [2], as shown in Fig. 1. The size of two crossed-dipoles is W_a to realize the operating frequency band. When one pair of dipoles works, the other pair acts as a parasitic unit to widen the antenna impedance bandwidth. Moreover, the antenna uses a rectangular ring radiator with two short-circuiting branches in the ring to change the current distribution on the surface of the antenna, which is conducive to the isolation degree between the two antenna ports. The total height of the antenna is H to meet the distance between the reflector plate and the bottom of the radiator is $1/4$ wavelength, which is beneficial to obtain the optimal unidirectional radiation performance of the antenna. What's more, the antenna is fed by probe coupling, as shown in Fig. 1 (c). The vertical part of the probe adds insulating dielectric and the horizontal part of the feed bar adopts the bending structure. There is a height difference between two feed bars, which also ensures to get the port high isolation characteristics.

In order to improve the performance of the antenna, we changed the plane reflector to a curved reflector (quadrilateral reflector). The reflector can make the backward radiated electromagnetic wave superimposed with the primary radiated electromagnetic wave after reflection to improve the antenna's directivity and gain.

The distance between the radiation and the reflector affects the directivity of the antenna. If the distance is too small, the pattern presents a single lobe, and the -3dB beamwidth is very narrow. However, if the distance is too large, the pattern presents multiple lobes, and the directivity of the antenna decreases. When the distance is between $0.3\sim 0.75\lambda$, the radiation resistance can be maximized, as the result, the antenna will obtain an optimal performance.

The length of the quadrilateral bottom reflector designed in this paper is W_{r2} , the length of the top side is W_{r1} , and the bending angle is 130° . The reflector is made of the same material as the antenna, and the thickness is 0.5 mm . Finally, this paper ultimately devised a quadrilateral bottom reflector which has a size

of $150\times 150\text{mm}$, showed in Fig. 1 (a). The specific design dimensions of the antenna are given in Table 1.

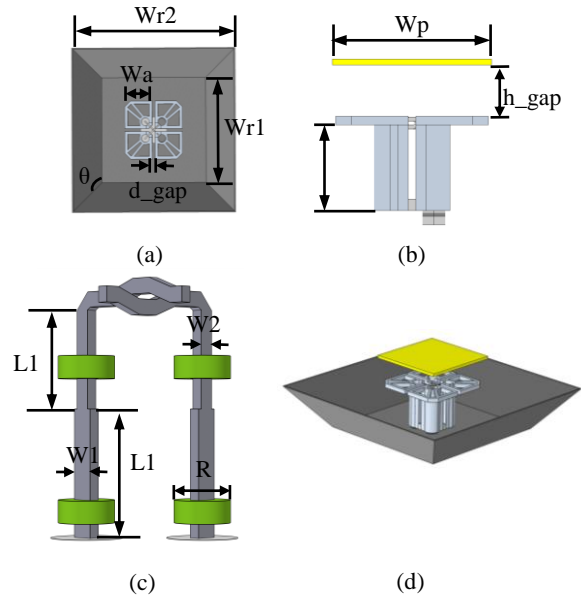


Fig. 1. Different configuration of the antenna. (a) With a quadrilateral reflector (top view). (b) With a PRMS structure (side view). (c) Structure of L-shaped probe. (d) With a quadrilateral reflector and PRMS structure.

Table 1: Geometric parameters of the antenna

Parameters	Value (mm)	Parameters	Value (mm)
W_a	23	L_1	12
W_{r1}	100	L_2	14
W_{r2}	150	D	7.5
W_1	3	d_gap	2.7
W_2	2	h_gap	18
W_p	56	h	33

B. Principle of PRMS structure

Nevertheless, the enhancement of antenna performance through the bottom reflector optimization is restricted. And the reflector can adversely affect impedance bandwidth. So, we used a partially reflective metasurface (PRMS) structure further.

Based on the principle of antenna energy radiation, the electromagnetic waves radiated from the feeder travel different distances to reach various positions on the partially reflective surface. Thus, the partially reflecting waves reflected multiple times have different reflection phases when they finally pass through the PRMS structure. Many studies have demonstrated that the reasonable phase compensation of the partially reflective surface can effectively broaden the gain bandwidth [21]. The phase bandwidth of the positive

reflection should match the working frequency band of the antenna as much as possible. Increasing the relative dielectric constant of the dielectric plate is a way to obtain a wider phase bandwidth, but increasing the thickness is directly equivalent to increasing the cost. Another method is to add an air gap between the ground plate and the dielectric plate of FSS [20],[22]. The substrate's energy bound is reduced because the low dielectric constant medium restricts the antenna radiation field less. Using this theory, the cell's phase change becomes gentler while the influence of surface wave is reduced.

C. Configuration of PRMS structure

In this section, a single-layer reflective metasurface structure with a square patch, a substrate and an air dielectric layer is designed. The side length of the patch is w , and the horizontal and vertical gap is g , as shown in Fig. 2. The patch unit cell is etched on one side of the dielectric board made out of a 2 mm thick FR4 substrate ($\epsilon_r = 4.4$, $\tan \delta = 0.018$). When electromagnetic waves are incident on the surface of the periodic metal patch, the induced current is excited at the same time, causing the gap between two adjacent patches to generate a coupling capacitance C .

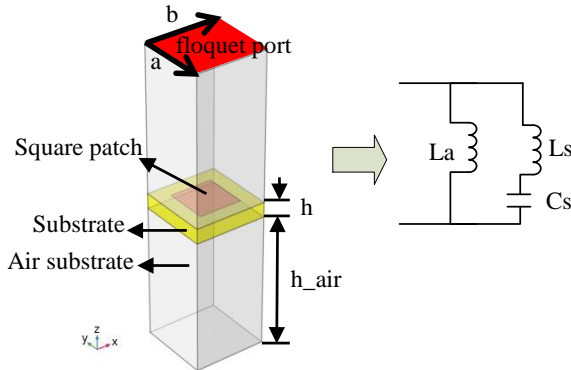


Fig. 2. Geometry settings of proposed metasurface unit and its equivalent circuit model.

The length of each patch generates an inductance, and the dielectric plate and the air layer generate the inductance is represented by L_a . Detailed equivalent circuit diagram of the partially reflective metasurface is shown in Fig. 3. Therefore, the total surface impedance can be expressed as [23]:

$$Z = Z_a // Z_s = j\omega L_a \frac{1 - w^2 L_s C_s}{1 - w^2 (L_s + L_a) C_s}, \quad (1)$$

where Z_s and Z_a are the equivalent impedances of the periodic patch and the total substrate, respectively, and the resonant frequency and reflection phase of the superstructure can be further calculated by the eq. (2):

$$f_s = \frac{1}{2\pi\sqrt{(L_s + L_a)C_s}}, \quad (2)$$

$$j\Phi = \ln \Gamma = \ln \frac{Z - \eta_0}{Z + \eta_0}, \quad (3)$$

where η_0 is the free space wave impedance.

Although the square patch generates the LC equivalent circuit structure in series, the high impedance characteristic at resonance makes the superstructure show in-phase reflection characteristics. The incident wave cannot achieve the ideal total reflection or complete transmission.

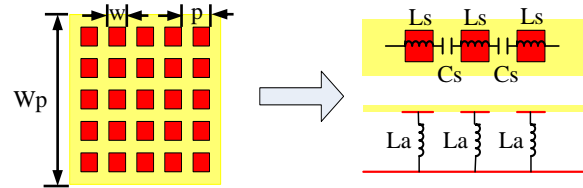


Fig. 3. Detailed equivalent circuit diagram of the partially reflective metasurface.

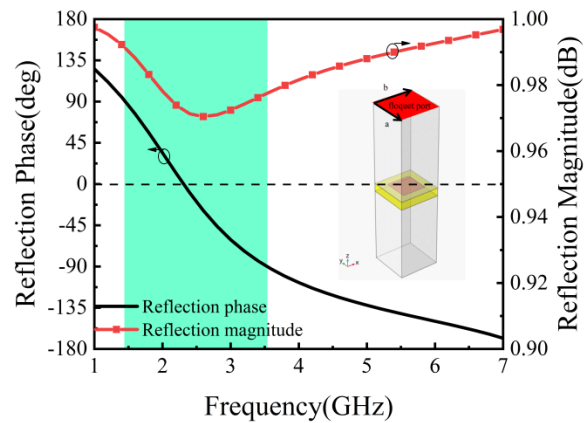


Fig. 4. Reflection phase and magnitude characteristics of the square patch metasurface. The blue band represents the $\pm 90^\circ$ reflection phase bandwidth, suggesting the operating frequency of the metasurface.

The Floquet port method of HFSS simulation software is used to simulate the PRMS structure. Modeling of a cell set up around the master-slave boundaries to simulate infinite cycle and setting the floquet port on the upper surface for excitation. The reflection coefficient amplitude for one cell on PRMS structure changes with frequency curve is shown in Fig. 4. In the working frequency band (1.5-3.5GHz), metasurface reflection coefficient is between 0-1, which can realize the part of the electromagnetic wave reflection. The incident electric field is basically all reflected, which meets the needs of resonant cavity

antenna. The designed PRMS structure in phase reflection bandwidth is basically consistent with the working bandwidth of the dipole antenna, thus the proposed structure can be used to improve the performance of the antenna.

Furthermore, the electromagnetic characteristics of metasurface are simulated by using CST. The electromagnetic wave incident to the near-zero refractive index metamaterial can be emitted almost perpendicular to the metamaterial surface and the antenna gain can be improved after the superposition of multiple reflected waves [19]. It can be seen from Fig. 5 that the magnetic permeability is close to zero at 3GHz. The relative permeability is $-0.12+j0.05$, which shows good space transmission performance of electromagnetic wave.

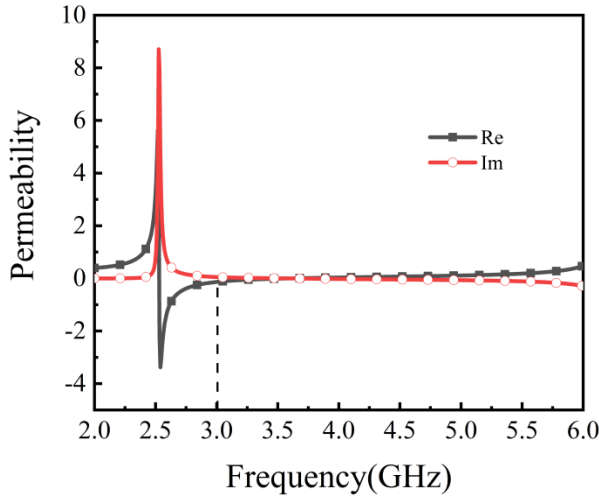


Fig. 5. Simulated permeability of metasurface unit.

III. OPTIMIZATION OF ANTENNA AND PRMS STRUCTURE

A. Analysis of the antenna parameter

The antenna is fed by a probe coupling, and the capacitance effect between the probe and the antenna radiator affects the working bandwidth of the antenna. Reasonable setting of the distance between the two can make the antenna achieve the best impedance matching. The simulation results of return loss under different spacing are shown in Fig. 6. It can be seen that with the increase of spacing, the capacitance value increases and the low-frequency resonance point gradually disappears. The impedance matching effect is the best when $R=3.75\text{mm}$. The spacing between dipole radiators also has a significant effect on antenna performance. When one pair of dipoles is excited, the other pair acts as a parasitic unit to extend the working bandwidth of the antenna, and the coupling current intensity can be adjusted by changing the distance between the dipoles. From Fig. 7, the simulated results show that the second

resonant point is closely related to the spacing. When d_{gap} is 1.7 mm, the antenna has only one resonant point. With the increase of d_{gap} , the value of the first resonant point moves up.

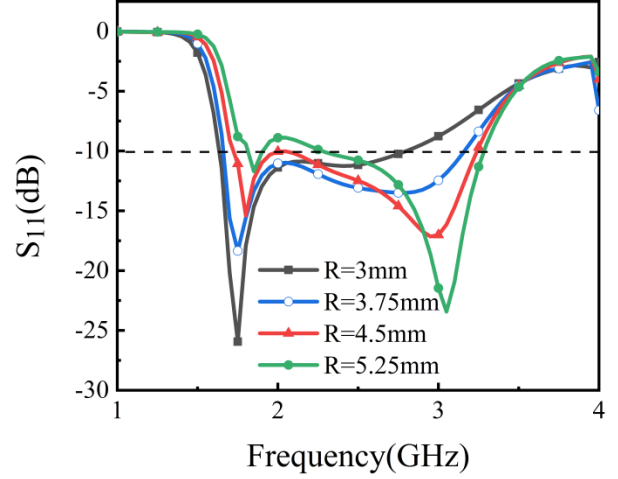


Fig. 6. Result of reflection with different R . The optimal bandwidth (1.67-3.17GHz) is achieved with $R=3.75\text{mm}$.

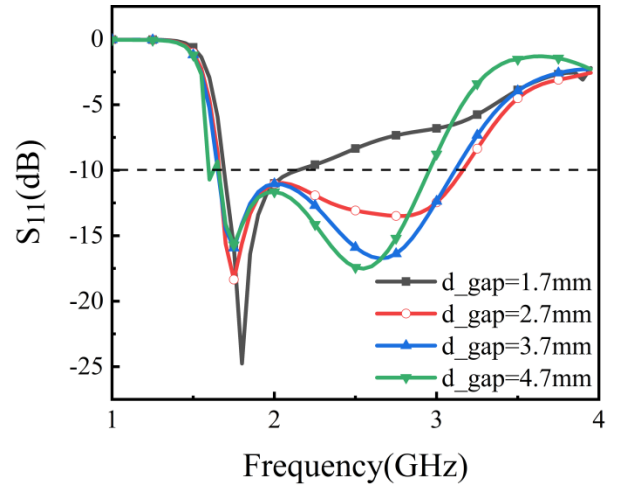


Fig. 7. Result of reflection with different d_{gap} . The optimal bandwidth (1.67-3.17GHz) is achieved with $d_{\text{gap}}=2.7\text{mm}$.

B. Optimization of the PRMS height

Electromagnetic waves are repeatedly reflected and transmitted through PRMS structure and the antenna, forming a resonant cavity. In the PRMS cavity, the antenna directivity coefficient (D_c) at the center frequency is indicated as follows [24]:

$$D_c = \frac{1+R}{1-R}, \quad (4)$$

where R is the magnitude of the PRMS reflection coefficient.

In the process of electromagnetic wave transmission, the signal energy in the resonant cavity is mitigated to different extend. The width of PRMS structure (W_p) and the height of PRMS structure (h_{gap}) all have great influence on the resonant cavity and then affect the antenna performance. We analysis two parameters (W_p and h_{gap}) separately.

The resonant point of the resonator cavity antenna is determined jointly by the height (h_{gap}), the reflecting phase of the PRMS structure (φ_1), and the reflective phase of the antenna bottom reflector (φ_2):

$$f = \frac{c}{2d} \left(\frac{\varphi_1 + \varphi_2}{2n} - n \right), n = 0, 1, 2, \dots, K. \quad (5)$$

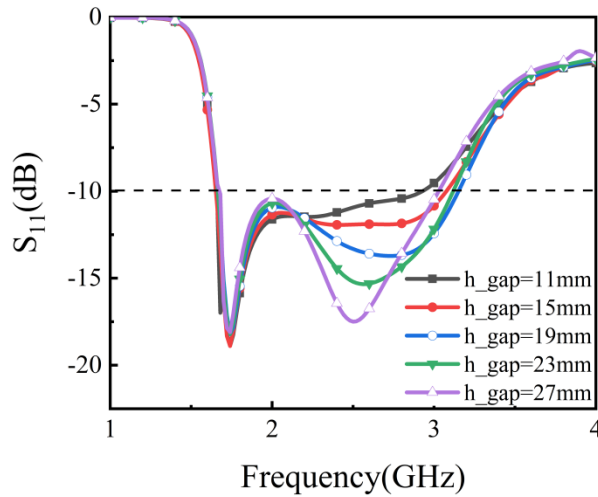


Fig. 8. Result of reflection with different h_{gap} . The optimal bandwidth (1.67-3.17GHz) is achieved with $h_{gap}=19$ mm.

The parameters were analyzed using Ansoft HFSS simulation software. The antenna bandwidth is essentially stable with the different distance between the PRMS and the antenna. Fig. 8 shows the S_{11} simulation results by changing the height h_{gap} . When $h_{gap}=19$ mm or 23mm, the -10dB impedance bandwidth of the antenna is 1.67 to 3.17GHz. Finally, Taking into account the size of the antenna, $d=19$ mm is the optimal height which was established in further research.

C. Optimization of the dimension of PRMS structure

The number of PRMS patch cell equal to the size of PRMS structure (W_p) also has an effect on bandwidth [16]. In this section, we first keep the height $h_{gap}=19$ mm is constant. After that, four groups of FSSs with varying cells which is 2×2 array ($W_p=30$ mm), 5×5 array ($W_p=56$ mm), 7×7 array ($W_p=80$ mm) and 9×9 array ($W_p=100$ mm) were chosen respectively to design the

reflector surface and combine with the dipole antenna.

Figure 9 shows the return loss simulation results. It is demonstrated that the size of PRMS structure has a great influence on the impedance bandwidth and the high frequency resonant point. The operating frequency band expands with the increase of PRMS dimension.

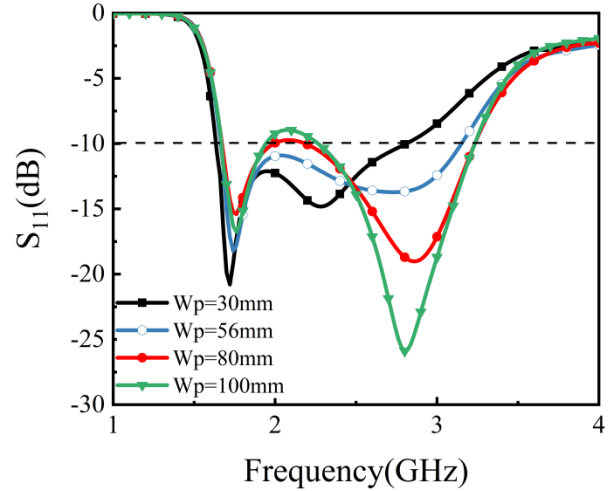


Fig. 9. Result of reflection with varying W_p . The widest -10dB impedance bandwidth is obtain when $W_p=56$ mm

IV. RESULTS

To better demonstrate the effect of designing PRMS structure, we have compared the return loss results of only antenna, adding PRMS structure, adding quadrilateral bottom reflector (Abbreviated in the figure as reflector), and antenna with PRMS and reflector. Fig. 10 shows the simulation result. It can be seen that the input impedance of the antenna changes after loading part of the reflected surface, resulting in the decrease of resonant frequency with the bandwidth is 1.67-3GHz. The maximum working frequency is reduced from 3GHz to 2.8GHz when the quadrilateral reflector is loaded. While the antenna added quadrilateral reflector and PRMS structure, the antenna has the best performance showing in a bandwidth increase of 61.2%.

Figure 11 shows the simulated results of antenna gain. The E-plane gain of antenna with PRMS structure is higher than that of antenna without PRMS structure within the operation band from 1.6-2.2GHz. Gain enhancement is very limited in other frequency. When the distance between antenna and metasurface is 18mm, the antenna gain increases significantly at 3GHz. The electromagnetic wave incident to the near-zero refractive index metamaterial can be emitted almost perpendicular to the metamaterial surface and the antenna gain can be improved after the superposition of multiple reflected waves. Adding quadrilateral reflector can effectively improve this deficiency. Moreover, the gain of the final proposed antenna is almost stable within the expect

frequency band. It can be seen from Fig. 12 that the antennas with PRMS structure have a higher cross-polarization ratio at low frequencies and the beamwidth is slightly reduced. The performance of antenna with different structure was compared in Table 2.

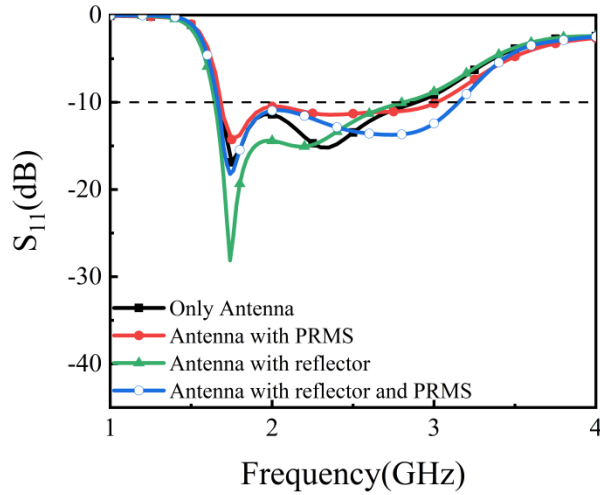


Fig. 10. Simulated reflection results with different antenna structure. Antenna with reflector and PRMS structure has the widest bandwidth.

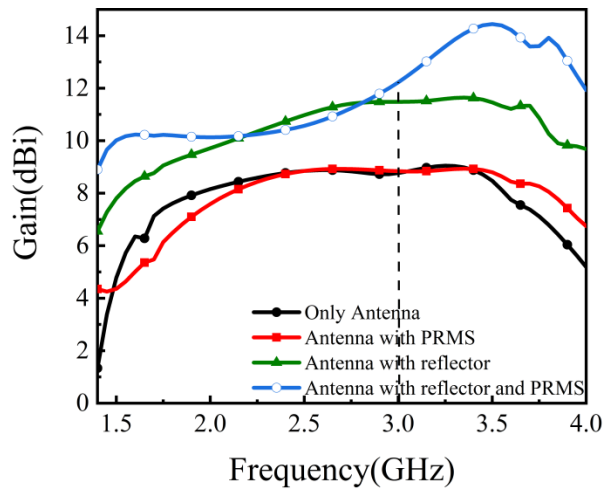


Fig. 11. Gain of antenna in E-plane in different antenna structure.

Therefore, we concluded that the gain enhancement method with PRMS structure is also efficiently to use in dipole antennas. The dipole antenna with PRMS structure is shown in Fig. 13. The space between the dipole antenna and the PRMS structure is supported by foam

which acts as an air dielectric layer.

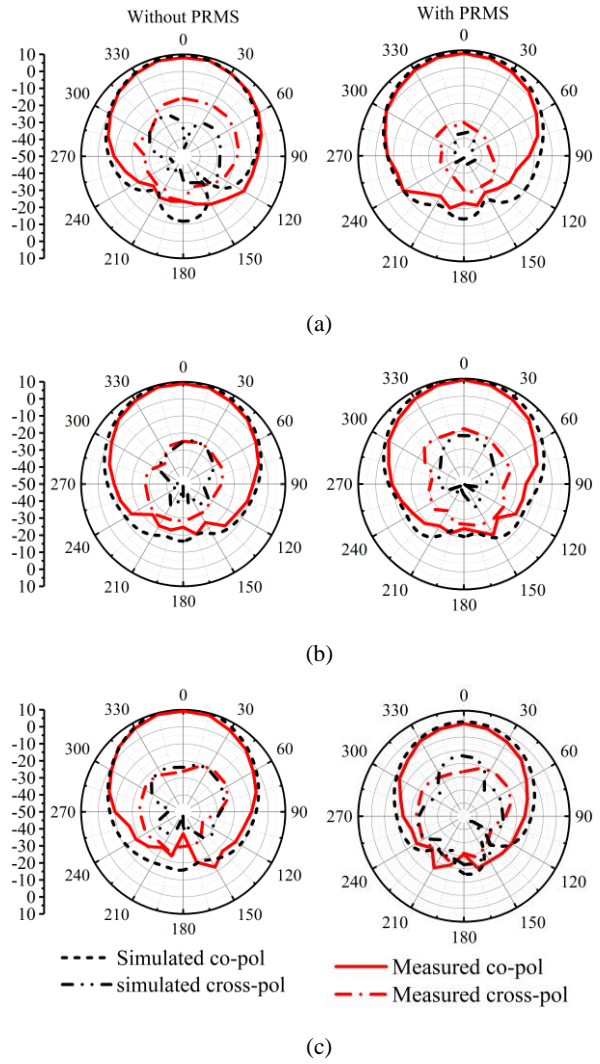


Fig. 12. Radiation patterns of the proposed metasurface antenna with reflector or without angular reflector at (a) 1.8GHz, (b) 2.2GHz, and (c) 2.8GHz.

Table 2: Comparison between the antenna with different structure

Antenna Structure	-10dB Bandwidth (GHz)	Gain at 3GHz (dBi)
Only antenna	1.6-2.8	7.6
Antenna with PRMS	1.6-2.97	7.6
Antenna with reflector	1.6-2.95	10.9
Antenna with reflector and PRMS	1.6-3.2	12.5

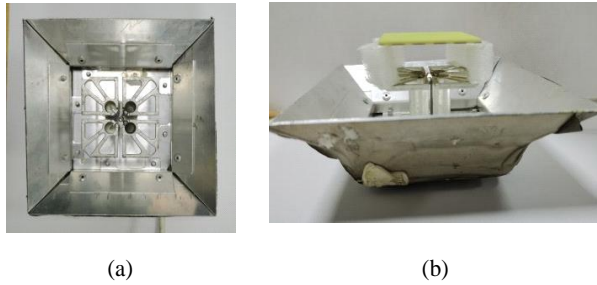


Fig. 13. (a) Fabricated dual-polarized dipole antenna (top view), and (b) fabricated proposed antenna with PRMS structure.

The actual measurement is basically consistent with the simulated return loss. Due to processing error and the simulation does not consider the influence of the four foam spacers supporting PRMS on the antenna performance, the resonant frequency has a deviation of 0.1 GHz, which can be ignored theoretically (Fig. 14). In this paper, the gain and direction of the design antenna is further measured and analyzed.

Furthermore, the performance of antennas with New Electromagnetic Materials is compared which are listed in Table 3. It is obvious that they have similar performance, but the proposed antenna has a smaller aperture size, which is benefit for using array antenna and coupling effect can be ignored.

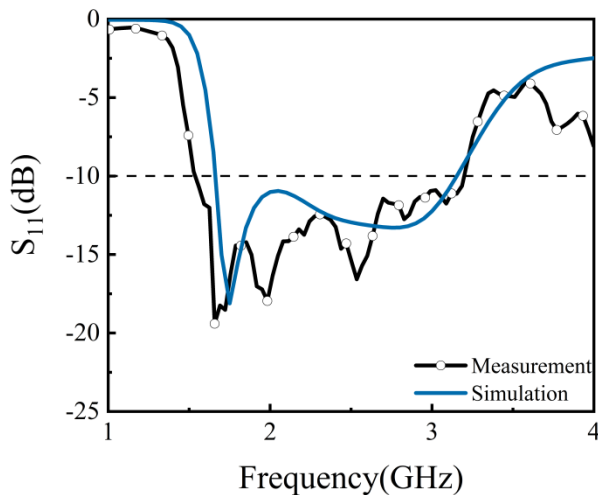


Fig. 14. Simulated and measured reflection results of proposed antenna.

Figure 15 shows the simulated and measured gain of the antenna. Because of the process error and test error, the measured gain is smaller than the simulation result. The measured efficiency is greater than 63% in the working frequency band, which meets the needs of practical engineering.

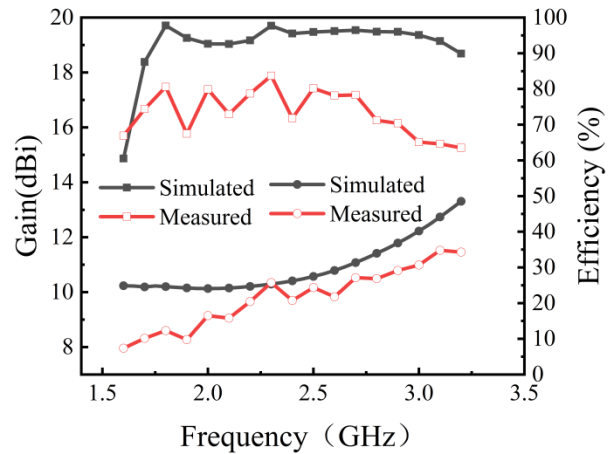


Fig. 15. Simulated and measured results of gain and efficiency.

Table 3: Comparison between the designed antenna and other high-gain antenna

Ref.	Antenna Type	-10dB Bandwidth (dB)	Maximum Gain (dBi)
[12]	Dual-polarized Fabry-Perot antenna	29.4% (8.7-11.7GHz)	15.7
[17]	Antenna Cavity resonator antenna	40.4% (8.1-12.2GHz)	12.5
[16]	Circularly polarized patch antenna	11% (2.34-2.64GHz)	9.1
[25]	Circularly polarized array	46.5% (1.9-3.05GHz)	12.8
This work	Dual-polarized dipole antenna	61.5% (1.6-3.1GHz)	12.7

Table 4: Comparison between the designed antenna and other base station antenna

Ref.	BW (GHz)	Isolation (dB)	Maximum Gain (dBi)	HPBW
[2]	1.7-2.7	>30	8.9	65.2±5.6
[3]	1.427-2.9	>20	8	66±3
[4]	4.5-5.0	>27	10.3	58±4
[5]	1.55-2.75 3.3-3.8	>30	7.6	68±5
[6]	1.71-2.71	>30	9.9	65±4.5
[7]	3.14-3.81	>43	12.5	64±3
This work	1.6-3.1	>28	12.7	65

As Table 4 shows the comparison between the antenna proposed in this paper and the existing base station antenna, it can be seen that the antenna proposed in this paper has a simple structure and the isolation degree meets the engineering needs while having the

highest gain. While the disadvantage is that the operating bandwidth cannot completely cover the Sub-6G band, and the future work we will further optimize the antenna so that it can be used as a 5G base station. Therefore, the proposed antenna has a wider field of application.

V. CONCLUSION

In this paper, a quadrilateral reflector and PRMS structure are used to design a broadband dual-polarized antenna. The principle of PRMS structure is analyzed by LC equivalent circuit. Then we properly design the dimensions of square patch and the thickness of substrate to optimize the performance of antenna. Moreover, the antenna gain is greatly improved by the combination of the quadrilateral bottom reflector and PRMS structure. The bandwidth of the final design has increase by 15.8%. In addition, the maximum gain has improved 4.9dBi at 2.8GHz and the efficiency in the working frequency band is greater than 63%. Therefore, the method we presented to enhance the gain and broaden the bandwidth is suitable for dipole antenna which makes it very attractive to different type of base station antenna array.

ACKNOWLEDGMENT

Thanks to the support of Qingdao University in 2021. Thanks to the National Key Research and Development Program Strategic International Science and Technology Cooperation and Innovation Program (2018YFE0206500) for its funding support.

REFERENCES

- [1] D. Z. Zheng and Q. X. Chu, "A wideband dual-polarized antenna with two independently controllable resonant modes and its array for base-station applications," *IEEE Transactions on Antennas and Propagation*, vol. 16, pp. 2014-2017, Apr. 2017.
- [2] Y. He and Y. Yue, "A novel broadband dual-polarized dipole antenna element for 2G/3G/LTE base stations," *2016 IEEE International Conference on RFID Technology and Applications (RFID-TA)*, Foshan, pp. 102-104, Nov. 2016.
- [3] Q. Zhang and Y. Gao, "A compact broadband dual-polarized antenna array for base stations," *IEEE Antennas and Wireless Propagation Letters*, vol. 17, no. 6, pp. 1073-1076, June 2018.
- [4] B. Qiu, S. Luo, and Y. Li, "A broadband dual-polarized antenna for sub-6 GHz base station application," *2020 IEEE 3rd International Conference on Electronic Information and Communication Technology (ICEICT)*, pp. 273-275, Dec. 2020.
- [5] Z. Li, J. Han, Y. Mu, X. Gao, and L. Li, "Dual-band dual-polarized base station antenna with a notch band for 2/3/4/5G communication systems," *IEEE Antennas and Wireless Propagation Letters*, vol. 19, no. 12, pp. 2462-2466, Dec. 2020.
- [6] H. Sun, C. Ding, T. S. Bird, and Y. J. Guo, "A base station antenna element with simple structure but excellent performance," *2018 Australian Microwave Symposium (AMS)*, pp. 35-36, Apr. 2018.
- [7] Y. Liu, S. Wang, X. Wang, and Y. Jia, "A differentially fed dual-polarized slot antenna with high isolation and low profile for base station application," *IEEE Antennas and Wireless Propagation Letters*, vol. 18, no. 2, pp. 303-307, Feb. 2019.
- [8] Q. Zhang, L. Si, Y. Huang, X. Lv, and W. Zhu, "Low-index-metamaterial for gain enhancement of planar terahertz antenna," *AIP Advances*, vol. 4, pp. 037103, Mar. 2014.
- [9] I. Yoo, M. F. Imani, T. Sleasman, and D. R. Smith, "Efficient complementary metamaterial element for waveguide-fed metasurface antennas," *Optics Express*, vol. 24, no. 25, pp. 28686-28692, Dec. 2016.
- [10] Y. Huang, L. Yang, J. Li, Y. Wang, and G. Wen, "Polarization conversing of metasurface for the application of wideband low-profile circular polarization slot antenna," *EJP Applied Metamaterials*, vol. 5, no. 11, pp. 1-13, Aug. 2018.
- [11] N. Nasimuddin, Z. N. Chen, and X. Qing, "Bandwidth enhancement of a single-feed circularly polarized antenna using a metasurface: Metamaterial-based wideband CP rectangular microstrip antenna," *IEEE Antennas and Propagation Magazine*, vol. 58, no. 2, pp. 39-46, Apr. 2016.
- [12] A. K. Singh, M. P. Abegaonkar, and S. K. Koul, "High-gain and high-aperture-efficiency cavity resonator antenna using metamaterial superstrate," *IEEE Antennas and Wireless Propagation Letters*, vol. 16, pp. 2388-2391, June 2017.
- [13] Z. Liu, "Effect of primary source location on Fabry-Perot Resonator antenna," *2009 Asia Pacific Microwave Conference*, Singapore, pp. 1809-1812, Sept. 2009.
- [14] K. L. Chung and S. Kharkovsky, "Metasurface-loaded circularly-polarized slot antenna with high front-to-back ratio," *Electronics Letters*, vol. 49, no. 16, pp. 979-981, Oct. 2013.
- [15] S. Chaimool, K. L. Chung, and Prayoot Akkaraekthalin, "Simultaneous gain and bandwidths enhancement of a single-feed circularly polarized patch antenna using a metamaterial reflective surface," *Progress in Electromagnetics Research B*, vol. 22, pp. 23-37, Jan. 2010.
- [16] S. Chaimool, K. L. Chung, and Prayoot Akkaraekthalin, "Bandwidth and gain enhancement of microstrip patch antennas using reflective metasurface," *IEICE Transactions Communication*, vol. E93-B, no. 10, Oct. 2010.
- [17] F. Qin, S. Gao, G. Wei, Q. Luo, and J. Xu, "Array-fed dual-polarized wideband Fabry-Perot antenna based on metasurface," *Microwave and Optical*

Technology Letters, vol. 58, no. 10, pp. 2316-2321, Mar. 2016.

- [18] L. Ji, Y. J. Guo, P. Qin, S. Gong, and R. Mittra, "A reconfigurable partially reflective surface (PRS) antenna for beam steering," *IEEE Transactions on Antennas and Propagation*, vol. 63, pp. 2387-2395, June 2015.
- [19] Y. Zhao, K. Yu, and Y. Li, "A high gain patch antenna using negative permeability metamaterial structures," *2017 Progress in Electromagnetics Research Symposium - Fall (PIERS - FALL)*, pp. 119-123, Nov. 2017.
- [20] D. Cure, T. M. Weller, and F. A. Miranda, "Non-uniform bias enhancement of a varactor-tuned FSS used with a low profile 2.4 GHz dipole antenna," *Proceedings of the 2012 IEEE International Symposium on Antennas and Propagation*, Chicago, IL, pp. 1-2, Sept. 2012.
- [21] F. Sultan and S. S. I. Mitu, "Superstrate-based beam scanning of a Fabry-Perot cavity antenna," *IEEE Antennas and Wireless Propagation Letters*, vol. 15, pp. 1187-1190, Nov. 2016.
- [22] J. Xue, W. Jiang, and S. Gong, "Wideband RCS reduction of slot-coupled patch antenna by AMC structure," *Electronics Letters*, vol. 53, no. 22, pp. 1454-1456, Dec. 2017.
- [23] M. Li, Q. L. Li, B. Wang, C. F. Zhou, and S. W. Cheung, "A low-profile dual-polarized dipole antenna using wideband AMC reflector," *IEEE Transactions on Antennas and Propagation*, vol. 66, no. 5, pp. 2610-2615, Dec. 2018.
- [24] T. Debogović and J. Perruisseau-Carrier, "Array-fed partially reflective surface antenna with independent scanning and beamwidth dynamic control," *IEEE Transactions on Antennas and Propagation*, vol. 62, pp. 446-449, Oct. 2014.
- [25] K. L. Chung, S. Chaimool, and C. Zhang, "Wideband subwavelength-profile circularly polarized array antenna using anisotropic metasurface," *Electronics Letters*, vol. 51, no. 18, pp. 1403-1405, Sept. 2015.
- [26] C. Wang, L. Zhang, S. Wu, S. Huang, C. Liu, X. Wu, "A Dual-band Monopole Antenna with EBG for Wearable Wireless Body Area Networks," *ACES Journal*, vol. 36, no. 1, pp. 48-54, Jan. 2021.



Chenqi Li was born on July 8, 1997. She received the B.S. degrees from Qingdao University, Qingdao, China, in 2019. She is pursuing M.S. degree in Signal and Information Processing from Qingdao University at present.

Her current research interests include base station antenna and

circularly polarized antenna. She attended the ICEICT Academic Conference in 2020.



Zhongsen Sun was born on July 11, 1980, in the P.R. of China. He received the M.S. and Ph.D. degrees in Radio Engineering from the Changchun Institute of Optics, Fine Mechanics and Physics, Chinese Academy of Sciences, 2004 and 2007 respectively. He received Professor in 2009. Winner of the award for the Best Scientific Work in Ministry of Industry and Information Technology of P.R. of China, 2018. His main research is in the area of Spectrum theory and radio communication.



Zhejun Jin received the B.S. degree in Electronics Engineering from the Yanbian University, China, in 2000, the M.S. degree in Electronics Engineering at Incheon University, South Korea, in 2006, and the Ph.D. degree from Hanyang University, Seoul, South Korea, in 2014. Since

September 2014, he has been an Assistant Professor at Qingdao University, China. His research interests are antennas, microwave circuit design, microwave component modeling, and wireless communication systems.



Tian Liu was born in 1989. She received the B.S. in Advanced Materials Engineering from Chungbuk National University, Korea, in 2013. The M.S. and Ph.D. Degrees in Materials Engineering (Electronic Material Lab.) from Chungbuk National University, South Korea, in 2015 and 2020. In 2020, she joined the College of Microtechnology and Nanotechnology, Qingdao University, China, as an Assistant Professor. Her current research interests include areas of frequency selective surface, metamaterial, metasurface absorbers and microwave absorbers.



Leonid F. Chernjgor Full Professor, Fellow of Commission B (Fields and Waves) in the Ukrainian National URSI Committee, Fellow of the Scientific Council for Physics of the Ionosphere in Ukraine, Vice-President of the Academic Council conferring the Candidate of Science

Degree (equivalent of American Ph.D.) and the Doctor of Science degree in Radio Science and a member of two other Academic Councils. Research Interests:

Nonstationary theory of the interaction between high-power radio emissions and near-earth plasmas. Large-scale (thousands of kilometers) perturbations launched by high-power HF and MF radio emissions in ionosphere-magnetosphere plasmas. Physical processes appearing in near-earth space from localized sources of energy of different physical nature (magnetic storms, solar terminator, solar eclipses, earthquakes, volcano eruptions, high-power explosions, rocket engine burns, etc.). Author and co-author of more than 700 scientific publications, including five science books and sixteen textbooks.



Yu Zheng received M.S. and Ph.D. degrees from V. N. Karazin Kharkiv National University, Kharkiv, Ukraine, in 1998 and 2006. Now he is working in College Electronic and Information, Qingdao University. In 2006 selected in corresponding member of Engineering Academy of Ukraine. His scientific interests include base Propagation of electromagnetic waves and RF technology.